 doi:10.20944/preprints201808.0005.v1

Article

Preparation, characterization, and sludge conditioning of cationic polyacrylamide synthesized by a novel UV-initiated system

Qingqing Guan[1,*], Guocheng Zhu [2], Yi Liao [c], Jin Xu [1], Xiaoxu Sun [1], Fang Tian [1], Jiaxing Xu [1] and Minghan Luo [1]

[1] Department of the Environmental Engineering, Nanjing Institute of Technology, 1 Hongjing Avenue, Nanjing 211167, People's Republic of China; wall@njit.edu.cn (Q.G.); xujin100408@163.com(J.X.); 253740501@qq.com(X.S.); 5696988@qq.com(F.T.); xujiaxing1987@163.com(J.X.); leon96201@163.com(M.L.)

[2] College of Civil Engineering, Hunan University of Science & Technology, Xiangtan, 411201, People's Republic of China; zhuguoc@hnust.edu.cn(G.Z.)

3 Department of Civil Engineering, Sichuan University of Science and Engineering, Zigong, Sichuan 643000, People's Republic of China; ly-001-1980@163.com(Y.L.)

* Correspondence: wall@njit.edu.cn ; Tel.: +86 25 86118973

Abstract: Controlling the concentration of free radicals in polymerization systems is advantageous for preparing cationic polyacrylamide (CPAM) with high molecular weight and acceptable dissolvability. In this study, a novel ultraviolet (UV)-initiated system characterized with adjustable light intensity and redox-azo complex initiator was used to synthesize a CPAM flocculant named NP. Comparatively, another CPAM flocculant named SP with stable UV light intensity and single initiator was prepared. The chemical structure, morphology, and thermal stability were analyzed through instrumental analysis. Proton nuclear magnetic resonance indicated that NP was successfully prepared, and a small fraction of cationic homopolymer was mixed in the product. Polymerization conditions were optimized, and polymerization mechanism was determined by investigating the effects of various parameters on intrinsic viscosity, conversion, and dissolvability. Results showed that the best performance was obtained at indexes of 0.45 wt‰ redox initiator concentration, 0.2 wt‰ azo initiator concentration, 40.0 wt% of cationic monomer, first- and second-stage light intensities of 8.5 and 13 mW/cm^2, respectively, and 3 wt% urea. Sludge conditioning performances of NP and SP were comparatively evaluated, and the mechanism was determined by investigating the sedimentation behavior and floc size distribution. High intrinsic viscosity, porous morphology structure, and the mixed cationic homopolymer of NP resulted in better sludge conditioning performance.

Keywords: polymer; characterization; sludge conditioning; UV; flocculant

1. Introduction

Considering that activated sludge process is an important treatment technology for a wide range of wastewaters, the high annual increase in excess sludge, representing 1% or 2% of treated wastewater and containing 50% to 80% of pollution, should be disposed. Sludge is difficult to dewater because small negatively charged particles are consistently distributed in the form of a stable colloidal suspension. Sludge conditioning prior to mechanical dewatering should be conducted to destabilize particulate systems[1-3].

In recent years, cationic polyacrylamide (CPAM) has been widely used for sludge conditioning because it can neutralize the surface charge of solid and bridge particles through its long polymer chain to form large flocs that can reduce specific resistance and cake compressibility of sludge [4-6]. The molecular weight (MW) of CPAM, which can be characterized by intrinsic viscosity, is closely related to bridging mechanism. With increasing polymer chain length, higher intrinsic viscosity leads to higher bridging performance, with numerous particles becoming involved [7]. Zheng et al. reported that a low filter cake moisture content (FCMC) was achieved with high-MW polymers under

 doi:10.20944/preprints201808.0005.v1

the same dosage of flocculants[5,6,8]. Zhu et al. determined that the best sludge dewatering performance is achieved by CPAM with the highest MW[4]. Zhou et al. indicated that the optimum dosage of CPAM is negatively correlated with its MW if the MW of CPAM reaches above 5 million[9]. Thus, studies focusing on the preparation technology of CPAM constantly optimize the MW synthesis conditions[10,11]. However, the dissolving time cannot be ignored although high-MW CPAM contributes to sludge dewatering. The dissolving time for existing CPAM products can reach several hours, a period considered long in practical applications[4]. Thus, MW and dissolving time of CPAM should be considered at the same time.

Dissolving time highly depends on molecular configuration. Commonly, CPAM will be nearly insoluble if molecular chains are cross-linked, whereas it will dissolve easily when the chain is linear[12]. The molecular configuration of CPAM is closely related to its polymerization. Radical concentration is a valuable tool to control organic polyelectrolyte chemical structure and achieve varying intrinsic viscosity and dissolving time. The concentration of free radicals at appropriate levels should be conducted appropriately as molecular chains will cross-link if the free radical concentration is high, whereas polymerization reaction cannot proceed at low levels. High-MW CPAM should be prepared to control the amounts of free radicals in polymerization systems. Agarwal et al. [13] investigated the graft copolymerization of guar-g-(acrylamide (AM)-co-diallyl dimethylammonium chloride) with cerous sulfate and potassium persulfate as complex initiators. The grafting ratio of grafted copolymer was higher than those of similar studies, as shown in reactions (1) and (2) (GG stands for guar gum):

$$Ce^{4+} + GG \rightarrow Ce^{3+} + GG \cdot, \quad (1)$$

$$S_2O_8^{2-} + 2Ce^{3+} \rightarrow 2SO_4^{2-} + 2Ce^{4+}. \quad (2)$$

A certain concentration of Ce4+ with initiating activity can be maintained in the polymerization system with the above reactions. Polymerization can be completely conducted; therefore, grafting ratio increases. Zhao et al. [14] prepared high-MW CPAM using redox materials and azo salt as complex initiators and controlled it to a low temperature for specific times; then, the prepared material was subjected to increasing temperature. The decomposition activation energy of redox initiators approximate 40 kJ/mol, whereas that of azo initiators reaches more than 100 kJ/mol[15,16]. Free radicals generated from redox initiator reaction under low temperature go copolymerization, whereas azo salt produces free radicals under high temperature when the redox initiator is exhausted. Therefore, high-MW CPAM polymerizes. However, polymerization and the effects of complex initiation on flocculant dissolvability have not been elaborated. The polymerization mechanism and control on radical concentration should be investigated. The aforementioned studies were initiated by heating, which is time consuming, energy consuming, and difficult to control[17]. Our previous research indicated that ultraviolet (UV) initiation features low reaction temperature, short polymerization time, high polymer MW, and environmental friendliness. UV light intensity can be altered immediately and easy to control[10,18]. In the present study, a novel UV initiating system characterized with adjustable light intensity and redox-azo complex initiators was established and used to prepare CPAM flocculant (NP) by maintaining a certain concentration of free radicals. Polymerization characteristics and mechanism of this novel complex UV initiation system were comprehensively determined by investigating the effects of various parameters on intrinsic viscosity, conversion, and dissolvability.

The primary objectives of this study are as follows: (1) to prepare NP with high intrinsic viscosity and acceptable dissolvability with this novel UV initiation system using AM and acryloxyethyltrimethyl ammonium chloride (DAC) as monomers; (2) to reveal the chemical structures, morphology, and thermal stability using Fourier transform infrared spectrometer (FT-IR), proton nuclear magnetic resonance spectrometer (1H NMR), thermogravimetry–differential scanning calorimetry (TG-DSC), and scanning electron microscopy (SEM); (3) to determine the polymerization mechanism and optimum preparation conditions by investigating the key aspects of initiating conditions, such as redox initiator concentration, azo initiator concentration, mass ratio between AM and DAC, urea concentration, light intensity at different stages on conversion, intrinsic

 doi:10.20944/preprints201808.0005.v1

viscosity, and dissolving time; (4) to evaluate NP sludge dewatering performance and mechanism by investigating dosage dependence, sedimentation behavior, and floc distribution.

2. Materials and Methods

2.1 Materials

The monomer AM (98.5%, w/w) was obtained from Lanjie Tap Water Co., Ltd (Chongqing, China). The cationic monomer DAC(80% in water) was supplied by Luyue Chemical Co., Ltd (Taian, China).The photo initiator 2,2'-azobis(2-methylpropionamide)dihydrochloride (V50) was obtained from Ruihong Biological Technology (Shanghai, China). AM, DAC and V50 were of industrial grade. The other reagents used in the experiments, including ammonium persulfate, sodium bisulfate ethanol, urea [$CO(NH_2)_2$], hydrochloric acid (HCl), and sodium hydroxide (NaOH), were of analytical grade. The purity of nitrogen gas was higher than 99.9%. All reagents were used directly without any further purification.

Table 1 Waste Sludge Characteristics

Moisture content(%)	Mass density(ml/g)	pH	Zeta potential(mV)	Conductivity(mS/cm)
98.9±0.15	0.989	7.38±0.14	-21.6±0.6	2.1±0.4

Raw waste sludge from the thickener of Jiangning Development Zone Drainage Co., Ltd. (Nanjing, China) was used for this study. The samples after collection were stored in a refrigerator maintained at 4 centigrade to minimize the microbial activity and analyzed within 3 days. The characteristics of the sludge are listed in Table 1.

2.2 Preparation method

The preparation device scheme is shown in Figure 1. The preparation of NP was performed as follows: AM, DAC, deionized water, and urea which acted as the cosolvent was first added to a reaction vessel made of silicate glass. Initiator V50, ammonium persulfate and sodium bisulfate were added during the purging of nitrogen gas for 30 min prior to UV activation. Through UV (main radiation wavelength between 300 and 400 nm, 365 nm) light intensity was controlled for a specific period and then turned to another intensity for a specific period, the flocculant was produced, and the aqueous solution was changed into a translucent colloid. The copolymers were purified with acetone and ethanol, followed by the process, of drying and grounding into powder.

The preparation procedure and conditions of SP, polyacrylamide (PAM) and poly(

Preprints (www.preprints.org) | NOT PEER-REVIEWED | Posted: 1 August 2018 doi:10.20944/preprints201808.0005.v1

acryloxyethyltrimethyl ammonium chloride) PDAC are referred to references[6,19].

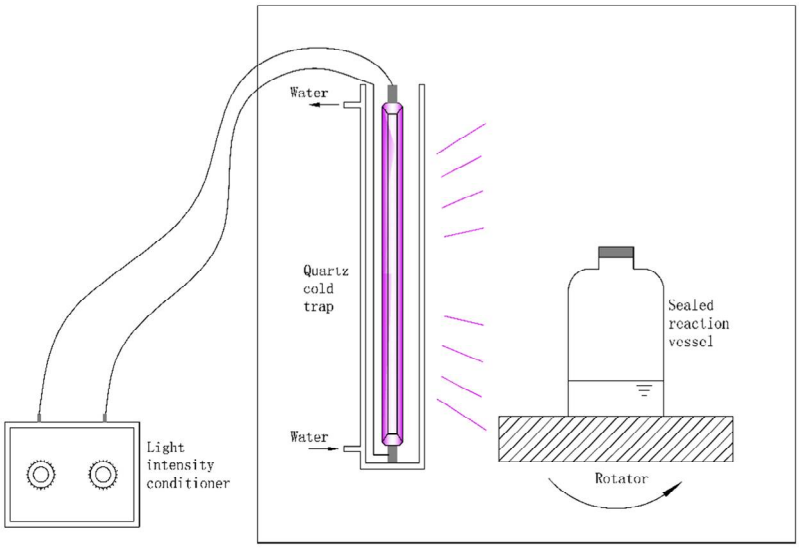

Figure 1. The preparation device scheme

2.3 Characterization of the Copolymer

The FTIR of the copolymer and monomers were conducted using a 550 Series II infrared spectrometer (Mettler-Toledo, Greifensee, Switzerland). The interval of the measured wave numbers was from 500 to 4000 cm^{-1}.

The ^{1}H NMR spectra of the flocculant were recorded on Bruker AVANCE-500 spectrometer (Bruker Company, Karlsruhe, Germany) in D_2O solvent.

TG-DSC was carried out at a heating rate of 10 °C/min, a nitrogen flow rate of 20 mL/min, and a temperature range of 20–600 °C on a DTG-60H synchronal thermal analyzer (Shimadzu, Kyoto, Japan).

Electron samples were prepared by shattering, planishing, and spraying. Then, the samples were dried, and SEM images were recorded on a VEGA II LMU instrument (TESCAN Company, Brno, Czech Republic).

The conversion and the intrinsic viscosity of NP or SP were determined by the gravimetric and one point method, respectively[11].The intrinsic viscosity was expressed in deciliter per gram(dL/g) and measured in 1.0 mol/L NaCl solution with an Ubbelohde capillary viscometer (Shanghai Shenyi Glass Instrument Co., Ltd., China) at 30 °C ± 0.05 °C.

The dissolving time was conducted as follows. About 0.04±0.002 g of the NP was added to a 200-mL beaker as the reaction vessel. Then, 100mL of distilled water was added into the reaction vessel, which was placed in an oscillator. The temperature of the oscillator was controlled at 30 centigrade while the electrode of conductivity meter was inserted into the beaker to determine whether the products completely dissolved or not. If conductance value did not change in 3 min, the sample was considered completely dissolved. Finally, the time required for complete dissolving the sample was recorded.

2.4 Sludge conditioning Experiment

Preprints (www.preprints.org) | NOT PEER-REVIEWED | Posted: 1 August 2018 doi:10.20944/preprints201808.0005.v1

In this study， Buchner funnel test was applied to examine the conditioning ability of the polymers[20]. The waste sludge was mixed by rapidly stirring at 200 rpm with paddle blade for 30 s in the presence of a certain dosage of copolymer solution (0.2%, wt). After 10 min settling period, residual turbidity (RT) sample was collected at 1 cm below the supernatant surface (Sinsche TB-2000, China). Zeta potential measurement (Zetasizer Nano ZS90, Britain) was referred to reference[20]. And the sludge floc size distribution was measured simultaneously (BT-9300H laser particle size distribution analyzer, Dandong Bettersize Instruments Ltd., China). The conditioned sludge was poured into a Buchner funnel to filter under a vacuum pressure of 0.05MPa for 30 min or until the vacuum could not be maintained (in <30 min). The filterability of the sludge is measured by Equation (3):

$$SRF = \frac{2bPA^2}{\mu\omega} \quad (3)$$

where SRF is the specific resistance of the sludge (m/kg); P is the filtration pressure (N/m^2); A is the filter area (m^2); μ is the viscosity of the filtrate (Ns/m^2);ω is the weight of cake solids per unit volume of filtrate (kg/m^3, $\omega=(1/C_i)/((100C_i-C_f)/100C_f)$; C_i is the initial moisture content(%); C_f is the final moisture content (%);b is the slope of filtrate discharge curve (t/V versus V) (s/m^6), where t is the filtration time (s) and V is the volume of the filtrate.

Filter cake moisture content (FCMC, %) of the conditioned sludge was determined using Equation (4):

$$FCMC = \frac{M_T - M_f}{M_T} \quad (4)$$

where M_T is the weight of filter cake after filtration (g) and M_f is the weight of filter cake after drying at 105 centigraded. The experiment was repeated three times and average results were reported. Settling rate tests were conducted in a graduated cylinder with 500 mL sludge sample. After 4 times inversion, the sludge suspension settled down without disturbance and the height of the sludge–liquid was recorded.

3. Results

3.1 Characterization

3.1.1 FT-IR spectra

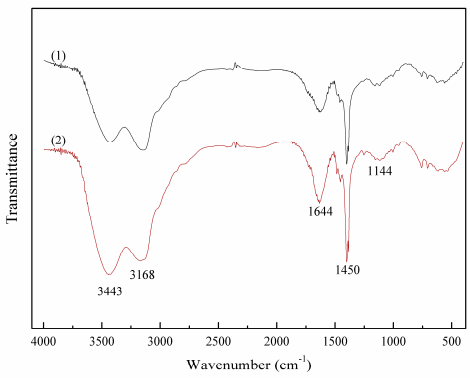

Figure 2. FT-IR spectra of (1)NP and (2)SP

Preprints (www.preprints.org) | NOT PEER-REVIEWED | Posted: 1 August 2018 doi:10.20944/preprints201808.0005.v1

Figure 2 shows the FT-IR spectra of NP and SP. Obviously, the adsorption peaks of NP and SP were almost the same, thus indicating that possible chemical bonds were the same. In other words, this novel UV initiating system didn't change chemical structures of copolymers. The adsorption peaks at 3443 cm^{-1}, 3168 cm^{-1} assigned to the stretching vibrations of $–NH_2$ in the amide groups. The adsorption peak at 1450 cm^{-1} represented for C=O in the amide groups. The adsorption peak at 1144 cm^{-1} corresponded to that of C-O in ester groups. The adsorption peak at 1450 cm^{-1} corresponded to CH_2- flexural vibrations in $-CH_2-N^+$. The adsorption peak at >3700 cm^{-1} stood for -OH stretching vibrations, indicating the overlapping broad and twin peaks. These overlapped peaks can be attributed to the small amount of bound water in the polymers as several chemical bonds were hydrophilic. The FT-IR spectra indicated that AM and DAC were reacted[18].

3.1.2 ^{1}H-NMR spectra

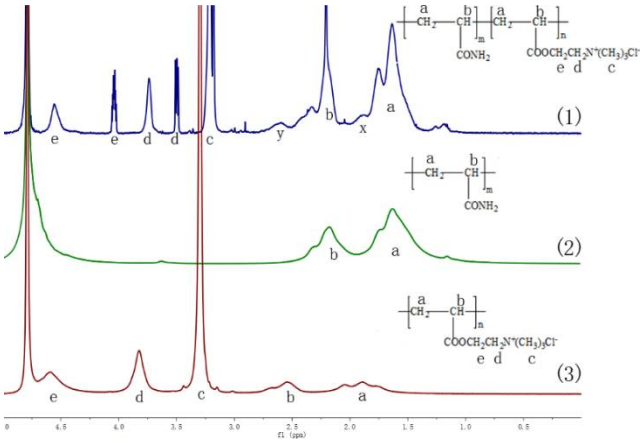

Figure 3. ^{1}HNMR spectra of (1) NP, (2) PAM, and (3) PDAC

Figure 3 shows the ^{1}H NMR spectra of NP, PAM, and PDAC. Several similarities were observed among NP, PAM, and PDAC, although the differences cannot be ignored. The asymmetric peaks of NP at δ = 1.64 ppm and sharp peak at δ=2.21 ppm were due to the protons at the backbone of methylene and methine groups-CH_2-(a) and -CH-(b), respectively. However, the protons in the structures of Figure 3(2) shifted to δ = 1.63 ppm and δ = 2.18 ppm, whereas the triplet and asymmetric peaks of -CH_2-(a) and -CH-(b) in Figure 3(3) shifted to δ = 1.89 ppm and δ = 2.54 ppm, respectively. The sharp peak at δ = 3.21 ppm in Figure 3(1) was assigned to the protons of -N^+-$(CH_3)_3$ (c) and was displayed at δ = 3.30 ppm in Figure 3(3). The peak of NP at approximately δ=3.74 ppm was assigned to the protons of -CH_2-N^+-(d), whereas it shifted to δ=3.89 ppm in PDAC. The chemical shift of NP at approximately δ = 4.66 ppm was ascribed to the protons of -O-CH_2-(e), and it shifted to 4.79 ppm in PDAC. These minor chemical shift differences for the same group among NP, PAM, and PDAC and the extra peaks indicated the successful preparation of NP using AM and DAC. The sharp peaks of the three polymers at δ = 4.79 ppm were identified as the solvent D_2O. Two more peaks at δ = 3.50 ppm and δ = 4.05 ppm, which were assigned to -CH_2-N^+-(d) and -O-CH_2-(e) in the ^{1}H NMR spectra of NP, respectively, were observed by comparing with PDAC spectra. Previous studies proposed that these extra peaks were attributed to the stereochemistry of the copolymers after copolymerization[21]. The chemical shifts in Figure 3(1) at approximately δ = 1.90 ppm （x） and δ = 2.59 ppm (y), which were not observed in ^{1}H NMR spectra of copolymers prepared by stable UV initiation system in our previous study[19], can be observed. The two peaks were nearly identical with those at δ = 1.89 ppm and δ = 2.54 ppm in Figure 3(3). This result indicated that a small fraction of PDAC homopolymer was mixed in NP. A probable explanation is proposed as follows: Our previous research indicated that the reactivity ratios of AM and DAC in solution polymerization are 2.27 and 0.38, respectively[19]. The conventional copolymerization equation, which describes the instantaneous copolymer composition and composition of the copolymer formed from a particular feed composition, was established by the reactivity ratios. This equation depicts that AM with high reactivity ratio significantly participated in copolymerization at

 doi:10.20944/preprints201808.0005.v1

the initial phase. In other words, the copolymers generated at such conditions featured low charge density (CD). The prepared polymers with high CD or PDAC can be obtained with continuous depletion of AM monomers. In our novel UV initiation system, DAC monomers can be sufficiently copolymerized with the complexation of different initiators with different activation energies and varying UV light intensities, that is, the radicals were distributed during copolymerization. Therefore, the copolymers generated at the end of polymerization exhibited high CD, or PDAC can be obtained. A small fraction of PDAC in NP copolymer caused the chemical shift at δ = 1.90 ppm （x） and δ = 2.59 ppm (y) in Figure 3(1). These PDAC homopolymers significantly contributed to sludge conditioning.

3.1.3 TG-DSC analysis

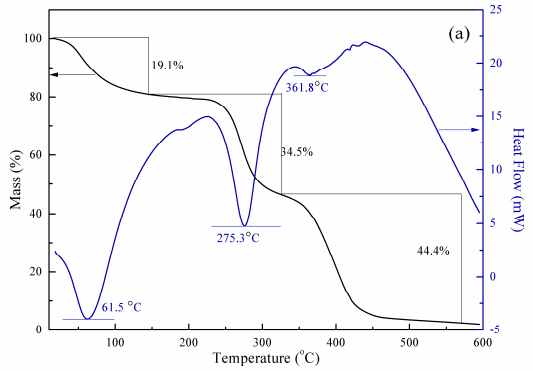

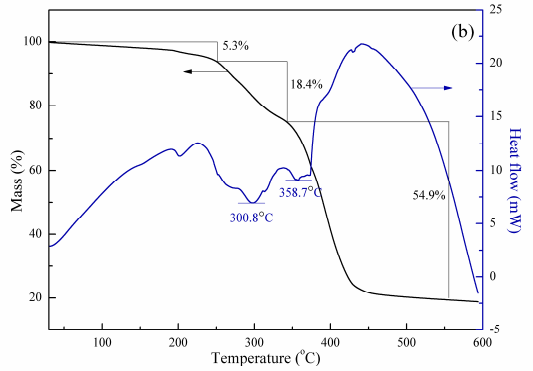

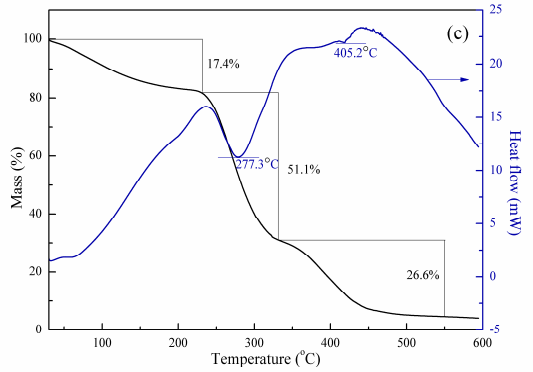

Figure 4. TG-DSC curves of (a) NP, (b) PAM, and (c) PDAC

 doi:10.20944/preprints201808.0005.v1

TG-DSC is commonly used to characterize the thermal stability of polymers by monitoring weight changes as a function of temperature. Figure 4 shows the TG-DSC curves of NP, PAM, and PDAC. The three main stages on copolymer thermal decomposition, which corresponded to weight reduction, were observed. In the initial stage, weight losses of approximately 19.1% (w/w) in the range of 20 °C–145 °C for NP, 5.3% in the range of 20 °C–250 °C for PAM, and 17.4% in the range of 20 °C–230 °C for PDAC occurred. The losses can be ascribed to the water molecules from air and which were absorbed by the hydrophilic groups of copolymers in polymerization. The water molecules vaporized at 100 °C, leading to a decrease in weight. During the second stage, weight losses of approximately 34.5%, 18.4%, and 51.1% were observed within the ranges of 145 °C–325 °C, 250 °C–340 °C, and 230 °C–330 °C, respectively. These losses corresponded to imidization of the amide group and thermal decomposition of methyl in the quaternary ammonium groups. All these polymers exhibited favorable thermal stability[22]. The final stage of thermal decomposition occurred above 325 °C, 340 °C, and 330 °C with weight losses of approximately 44.4%, 54.9%, and 26.6%, respectively. These weight losses were due to thermal decomposition of the polymer backbone. As shown in Figure 4, the heat adsorption peak of NP at the final stage reached 361.8 °C, which was between those of PAM and PDAC. Such result also indicated that AM and DAC had been successfully copolymerized.

3.1.4 SEM

 doi:10.20944/preprints201808.0005.v1

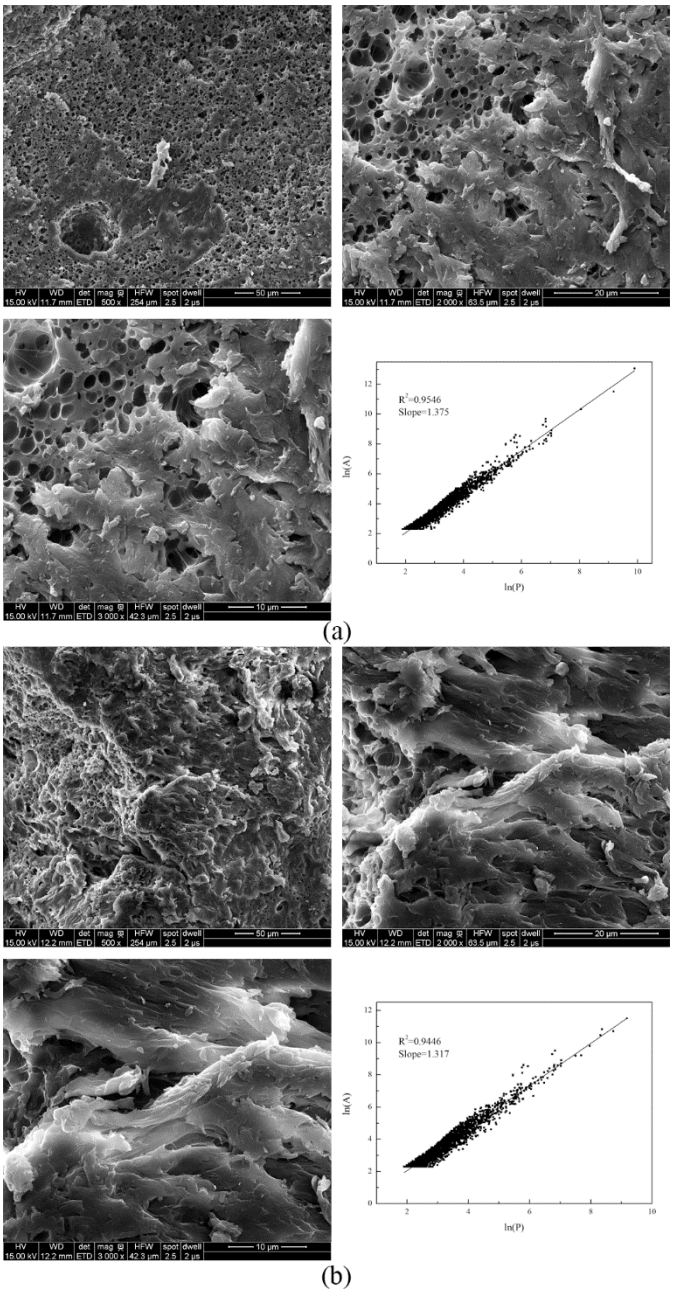

Figure 5. SEM images of (a) NP and (b) SP

Figure 5 illustrates the SEM images of NP and SP. Two different surface morphologies were observed. NP presented a porous structure with a prodigious surface area (Figure 5(a)), whereas the surface structure of SP was less porous (Figure 5(b)). In addition, Figure 5 also displays the linear correlation of the natural logarithms of the perimeter (L) and the area (A), indicating that the fractal dimension of the polymer surface could be calculated using Image-Pro Plus 6.0 software. Fractal dimension refers to the slope of the fitted curve. The results showed that the fractal dimensions of NP and SP were 1.375 and 1.317, respectively. The morphological structure of NP resulted in several kinds of surface modification induced by the novel UV initiation system. The porous structure favored water penetration in the polymeric network. Thus, product solubility can be improved. Previous studies have indicated that such structure favors flocculation of colloidal particles and formation of bridge aggregation among flocs. Compared with the smooth structure, such porous structure proves better for adsorption-bridging behavior between the flocculants and particles in sludge dewatering[5,23].

3.2 Synthesis condition optimization

Preprints (www.preprints.org) | NOT PEER-REVIEWED | Posted: 1 August 2018 doi:10.20944/preprints201808.0005.v1

3.2.1 Effect of initiator concentration on copolymerization

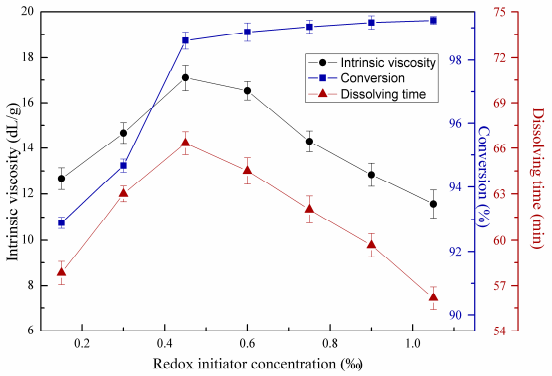

Figure 6 Effects of redox initiator concentration on copolymerization

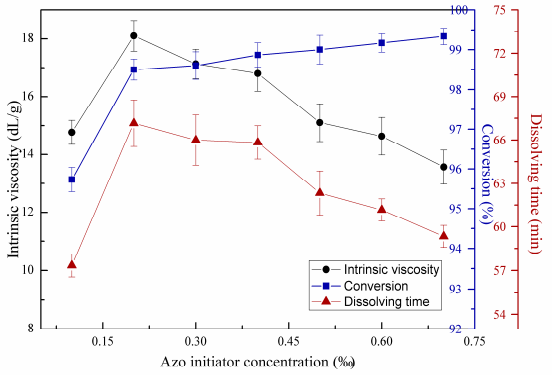

Figure 7 Effects of azo initiator concentration on copolymerization

Figure 6 illustrates the effects of redox initiator concentration on copolymerization using first-stage light intensity of 7 mW/cm², second-stage light intensity of 14.5 mW/cm², mass ratio between AM and DAC of 7:3, urea concentration of 2 wt‰, and azo initiator concentration of 0.3 wt‰. Figure 7 shows the effects of azo initiator concentration on copolymerization under the same reaction conditions in Figure 6, except that redox initiator concentration equaled 0.45 wt‰. Copolymer intrinsic viscosity and dissolving time increased with increasing initiator concentration after reaching maximum at redox initiator of 0.45 wt‰ and azo initiator concentration of 0.2 wt‰ but decreased with further increase in initiator concentration based on Figures 6 and 7. Conversion continually increased in the entire initiator concentration range, featuring a notable decreasing speed. Seabrook et al. proved that classical free-classical polymerization kinetics provides an acceptable quantitative description for photo-initiated polymerization of AM in water[24]. This phenomenon occurs due to the complex formation, cage effect, or primary radical termination with macro-radicals. When the redox or azo initiator concentrations were insufficient, the cage effect may lead to low polymer yields and low intrinsic viscosity due to the predominating termination of growing chains inside the cage as few monomer units contributed to propagation. Considerable primary radicals escaped from their “cages” to react with monomers, leading to the continuous growth of molecular chain with increasing initiator concentrations. At this condition, conversion also increased remarkably. However, chain termination and transfer will occur more easily with increasing redox initiator concentration above 0.45 wt‰ and azo initiator concentration above 0.2 wt‰ as radical concentration in the polymerization system increased[25]. This trend accorded well with the classical kinetic theory, which predicts that kinetic chain length depends on the square root of initiator concentration. Additionally, monomers still feature high chances to convert into

Preprints (www.preprints.org) | NOT PEER-REVIEWED | Posted: 1 August 2018 doi:10.20944/preprints201808.0005.v1

copolymers with the numerous produced radicals. The gel effect hampered the increase in monomers without limitation[26].

3.2.2 Effects of mass ratio between AM and DAC on copolymerization

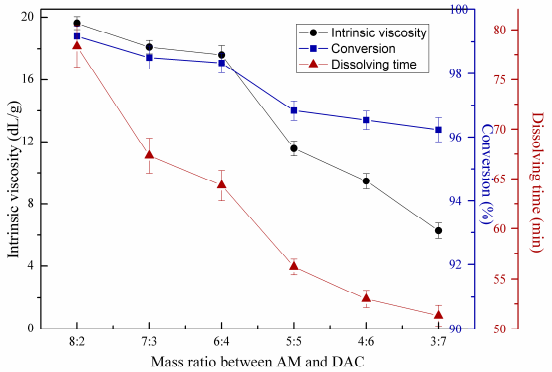

Figure 8 Effects of mass ratio between AM and DAC on copolymerization

Figure 8 shows the effects of mass ratio between AM and DAC on copolymerization. The experiment was conducted with 0.45 wt‰ redox initiator concentration, 0.2 wt‰ azo initiator concentration, 7 mW/cm² first-stage light intensity, 14.5 mW/cm² second-stage light intensity, and urea concentration of 2 wt‰. CPAM features wide applications because it can neutralize the surface charge of colloid particles to form large flocs. Charge density is directly related to charge neutralization efficiency and flocculation performance. However, intrinsic viscosity, conversion, and dissolving time all decreased with increasing DAC ratio, as shown in Figure 8. As mentioned above, the reactivity ratio of AM was higher than that of DAC in solution polymerization[19]. DAC monomers were less likely to polymerize with increasing molecular chains than AM monomers. In addition, the large steric hindrance and cationic charge repulsion caused by the quaternary ammonium groups in DAC caused difficulty in preparation of copolymers with ultrahigh intrinsic viscosity and conversion [6]. However, the dissolving time of produced copolymers decreased with increasing DAC mass ratio, facilitating their application in water treatment. The hydrophilic quaternary ammonium groups in DAC and low intrinsic viscosity resulted in the above phenomena. The intrinsic viscosity of 6:4 mass ratio was lower than that of 7:3 mass ratio, but better charge neutralization performance and shorter dissolving time were expected. Thus, in this study, the optimum mass ratio between AM and DAC was 6:4.

3.2.3 Effects of urea concentration on copolymerization

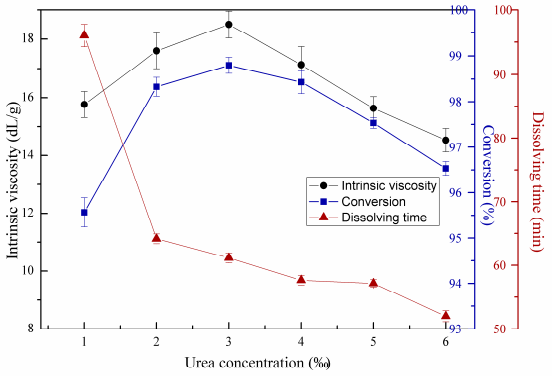

Figure 9 Effects of urea concentration on copolymerization

Preprints (www.preprints.org) | NOT PEER-REVIEWED | Posted: 1 August 2018 doi:10.20944/preprints201808.0005.v1

Figure 9 illustrates the effects of urea concentration, where the redox initiator, azo initiator, first-stage light intensity, second-stage light intensity, and mass ratio between AM and DAC reached 0.45 wt‰, 0.2 wt‰, 7 mW/cm², 14.5 mW/cm², and 6:4, respectively. As mentioned above, short dissolving time will facilitate the actual CPAM application. However, significant differences in size and velocity between the water and polymer inhibited water to seep in the polymer molecular chain of the copolymer solution. Urea can weaken hydrogen bonding between the side groups of CPAM molecular chain, resulting in the decreased intermolecular forces and chance of crosslinking. Therefore, urea was used as solubilizer in polymerization to reduce the dissolving time. Despite the decreased dissolving time with increased urea concentration, urea influenced intrinsic viscosity. This condition was observed as urea acted as a reducing agent to increase the kinetic chain length, and this effect can be observed when urea concentration measured below 3‰. However, the negative effect of urea is that it can transfer growing chains to cause radical termination, thus decreasing intrinsic viscosity and conversion. As shown in Figure 9, in the present study, the optimum urea concentration reached 3 wt ‰.

3.2.4 Effects of light intensity on copolymerization

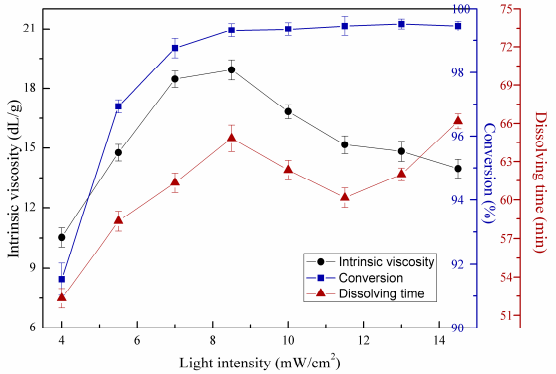

Figure 10 Effects of first-stage light intensity on copolymerization

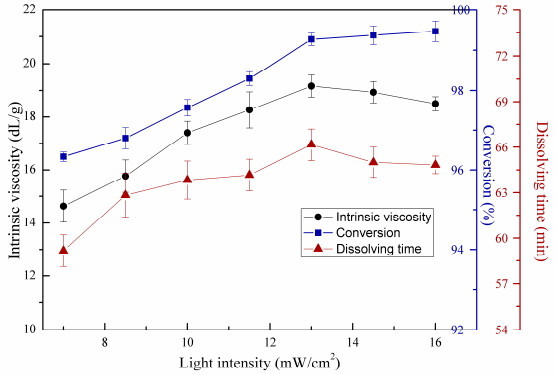

Figure 11 Effects of second-stage light intensity on copolymerization

Figure 10 shows the effects of first-stage light intensity on copolymerization. As shown in the figure, second-stage light intensity, redox initiator concentration, V-50 concentration, mass ratio between AM and DAC, and urea concentration totaled 14.5 mW/cm², 0.45 wt‰, 0.2 wt‰, 6:4, and 2 wt‰, respectively. Figure 11 shows the effects of second-stage light intensity on copolymerization under the same reaction conditions in Figure 10, except that the first-stage light intensity measured 8.5 mW/cm². As shown in Figure 10, the intrinsic viscosity, conversion, and dissolving time of copolymer all increased with increasing first-stage light intensity from 4 mW/cm² to 8.5 mW/cm². However, intrinsic viscosity immensely increased, conversion ratio constantly remained, and

 doi:10.20944/preprints201808.0005.v1

dissolving time decreased, reached a bottom, and increased again with increasing first-stage light intensity. These trends can also be illustrated by the radical copolymerization theory. Initiators can be decomposed and used to generate primary free radicals by UV light. Free radical concentration is positively correlated with UV light intensity[5]. Therefore, intrinsic viscosity and conversion (Figure 10) presented a similar trend with those in Figures 6 and 7. The cage effect may lead to low copolymer yields when light intensity is relatively low[23]. The increase in light intensity above 8.5 mW/cm^2 will increase termination and chain transfer rate, leading to decreased intrinsic viscosity. Accordingly, the first-stage light intensity reached 8.5 mW/cm^2. Monomers can be adequately copolymerized with increasing radical concentration. Therefore, conversion still increased when light intensity was above 8.5 mW/cm^2. In addition, the dissolving time showed different trends with intrinsic viscosity when light intensity increased above 13 mW/cm^2. The molecular chain may be slightly cross-linked, thus increasing the dissolving time in Figure 10. These results indicate that dissolving time mainly relies on intrinsic viscosity when cross-linking is small.

As shown in Figure 11, the curves showed similar trends with those in Figure 10. Intrinsic viscosity and dissolving time increased and decreased with increasing second-stage light intensity, and conversion followed a continuously increasing trend. The highest intrinsic viscosity was observed at second-stage light intensity of 13 mW/cm^2. However, differences were observed between the two figures. First, in Figure 11, no vast decreasing range was observed in intrinsic viscosity after reaching the maximum. Second, the dissolving time still correlated well with intrinsic viscosity although light intensity was higher than 13 mW/cm^2, indicating that the copolymer was not cross-linked at such condition. Different polymerization stages caused the above differences. The increasing second-stage light intensity below 13 mW/cm^2 contributed to high conversion and increase in intrinsic viscosity. However, after the first-stage UV illumination, a certain number of monomers were reacted, and a gel product can be produced. The radical concentration at the middle or last phase will not reach as high as that in the initial phase with the same light intensity given that radical concentration is influenced by monomer concentration. As mentioned above, chain termination and transfer rate were directly affected by radical concentration. Therefore, intrinsic viscosity was less influenced by increasing light intensity above 13 mW/cm^2, and molecular chain cross-linking was also less likely to occur.

3.2.5 Mechanism and advantages of the novel UV initiation system

Table 2 NP and SP characteristics at optimum condition

Polymer	Intrinsic viscosity (d L/mg)	Dissolving time (min)	Conversion (%)	CD (w/w)	Unreacted DAC monomer*	Unreacted AM monomer*
NP	19.2	66	99.3%	39.6%	0.4%	0.3%
SP	18.3	72	95.1%	35.8%	4.2%	0.7%

*The unreacted DAC percentage is obtained by 40% (total DAC monomer percentage) minus CD. The unreacted AM percentage is obtained by 100% minus conversion and unreacted DAC percentage.

As shown in Table 2, the intrinsic viscosity of NP was higher than that of SP, whereas the dissolving time of NP was lower than that of SP. These findings indicated that NP flocculated more efficiently and was more applicable than SP. The differences between the initiation systems resulted in the above experimental results. First, radical concentration was differently distributed during polymerization. Chain termination and transfer rate, which were directly affected by radical concentration, resulted in a decisive effect on copolymer intrinsic viscosity. In the novel UV initiation system, most redox initiators with low activation energy reacted to produce radicals at the first low-light-intensity stage of copolymerization, and most azo initiators with high activation energy decomposed in the second light stage. Radicals were generated and controlled at relatively low levels during the entire copolymerization. On the contrary, radicals cannot be generated nor regularly distributed during copolymerization in traditional stable light intensity and single UV

 doi:10.20944/preprints201808.0005.v1

initiation system. Chain termination and transfer rate of our novel UV initiation system were lower than those of SP. Second, radicals were insufficient to polymerize all the monomers for the stable light intensity system as the initiators were exhausted at the end of polymerization. Notably, the initiator concentration should be low because cross-linking will occur due to high concentration of radicals. By contrast, radicals can still be generated with increasing light intensity, which can lead to decomposition of azo initiators. Therefore, the monomers were sufficiently polymerized in this novel UV initiation system, as shown in the conversion rates in Table 2. Table 2 also shows that the CD of NP was significantly higher than that of SP. As mentioned above, the reactivity ratio of DAC is lower than that of AM[19]. In other words, the polymerization activity of DAC was insufficient for complete reaction in a single initiator and stable light intensity system. As shown in Table 2, the unreacted percentage of DAC monomer reached 4.2% for SP, whereas that of NP totaled 0.4%. This finding indicated that the novel UV initiation system is efficient and cost-effective. In addition, the extra 3.8% was converted to PDAC considering the ^{1}H NMR spectra of NP in Figure 3. This PDAC will significantly facilitate sludge conditioning. Third, the increasing light intensity of the novel UV initiation system can mitigate the gel effect in inhibiting radical generation. Monomers are transferred into copolymers, and a gel product can be produced with copolymerization. Light intensity decreased along the radiation path due to light absorption of initiator and scattering effect in reaction medium. This variance will lead to the spatially inhomogeneous distribution of free radicals in the system. Thus, conversion rate and intrinsic viscosity of various layers in the reaction vessel differed in the stable UV light intensity system. However, in this study, a closely homogeneous distribution of free radicals can be achieved by increasing the utilized UV light intensity. Consequently, monomers in different radiation paths can be copolymerized thoroughly, and average conversion rate and intrinsic viscosity increased.

For the low dissolving time of NP, the low possibility of copolymer chain cross-linking may explain why this experimental result was obtained although the intrinsic viscosity of NP was high. As mentioned above, radicals were generated and controlled during polymerization through different initiators and light intensities used in our novel UV system. Therefore, radical concentration was controlled at low level during copolymerization, and cross-linking was avoided. In addition, a porous morphology favored water penetration in the polymeric network structure based on Figure 5. Therefore, NP was dissolved better than SP.

The implications of our novel UV initiation system bear significance. One of the major obstacles in applying UV initiation technology in preparing organic flocculants is the light-hindering effect of gel product. The heterogeneous distribution of free radicals along the radiation path may pose a negative effect on polymerization. Such effect is unremarkable in laboratory-scale as the radiation path is often short. However, the hindering effect cannot be ignored in large industrial scale. The novel UV initiation system makes it theoretically possible by increasing light intensity and complexing of initiators with different activation energies.

3.3 Sludge conditioning performance and mechanism

3.3.1 Effects of flocculant dosage on sludge conditioning performance

 doi:10.20944/preprints201808.0005.v1

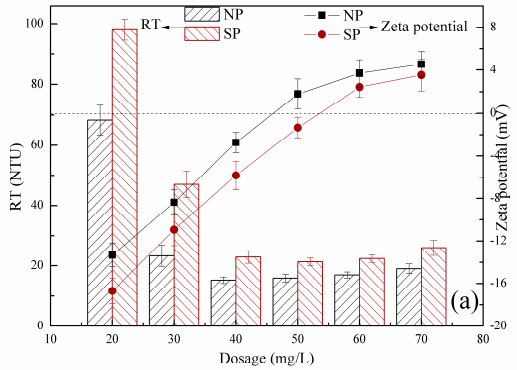

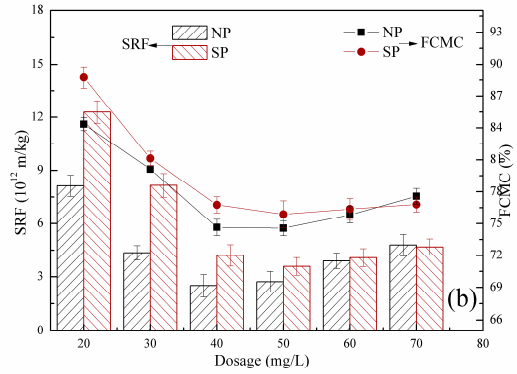

Figure 12. Effects of NP and SP dosages on residual turbidity (RT) and zeta potential (a), FCMC and SRF (b)

The conditioning efficiency of flocculants is influenced by a number of external factors, such as flocculant dosage. Turbidity is widely used to explain the performance of a polymer sample in various flocculation fields because it indicates the content of suspended particles in the liquid phase. FCMC is an important aspect to be considered in compressible sludge dewatering. High FCMC is not desirable because it results in large sludge volumes that increase the following treatment costs. SRF is widely used to evaluate sludge filtration performance, and small SRF reflects a good performance in sludge dewatering. Zeta potential plays an important role in analyzing the charge interactions between the polyelectrolyte and oppositely charged particles[20]. Figure 12 shows the effect of NP and SP dosages on RT, zeta potential, FCMC, and SRF. Clear solid–liquid separation was achieved when the dosage was higher than 40 mg/L for NP and SP, as shown in Figure 12 (a). This result corresponded well with that of FCMC and SRF, as shown in Figure 12 (b). Such experimental results indicated that the optimum dosage was 40 mg/L for the two polyelectrolytes. NP constantly showed lower ratios of RT, FCMC, and SRF than SP. A good sludge conditioning performance of NP was obtained, and this condition was closely related to CD, intrinsic viscosity, and morphological porous structure.

The indices RT, FCMC, and SRF for the two flocculants rapidly decreased with increasing flocculant dosage, gradually reached the minimum, and slowly increased with increasing flocculant dosage, respectively. These trends were consistent with the typical behavior of polyelectrolytes in the flocculation process reported in previous studies. The trends in the three indices corresponded with the changes in zeta potential of the supernatant in Figure 12 (a). The negative charge on the sludge surface was gradually neutralized, and colloid particles in the sludge destabilized and aggregated with the addition of positively charged flocculants. Correspondingly, the RT, FCMC, and SRF all decreased. High CD of NP favored charge neutralization as numerous cationic sites

 doi:10.20944/preprints201808.0005.v1

were provided. Negatively charged sites of sludge particles were sufficiently neutralized, and good conditioning performance may be achieved. This finding was ascertained by the high zeta potential of NP in Figure 12 (a) and initially explains the good conditioning performance. Charge neutralization was the main mechanism when the most favorable flocculation performance occurred at various flocculant dosages, where zeta potential was zero or close to zero. The repulsive forces between suspended charged particles nearly diminished, and efficient flocculation occurred, leading to effective sludge conditioning. However, in this study, zeta potential was lower than zero at a dosage of 40 mg/L, that is, the optimum dosage. This finding proves bridging, which is relatively common for high intrinsic viscosity polyelectrolytes. The porous morphological structure of NP with a prodigious surface area can crucially enhance the adsorption of polymers on particle surfaces and bridging of particles by polymer chain. In addition, the intrinsic viscosity significantly affects sludge conditioning. At high intrinsic viscosity, the flocculant presented an expanded chain conformation, and molecular chain stretching in the solution was sufficiently long to capture and bridge the colloidal particles [27,28]. An increase in intrinsic viscosity led to molecular chain growth, increased the chance of collision among the colloidal particles, and favored trapping and bridging of particles[29,30]. Therefore, the sludge conditioned by NP was flocculated. Excess flocculants can cause an electrostatic repulsion or a steric effect between the sludge particles, leading to restabilization of sludge particles, a condition that is not conducive to sludge dewatering, as shown in Figure 12.

3.3.2 Sludge floc properties and flocculation mechanism

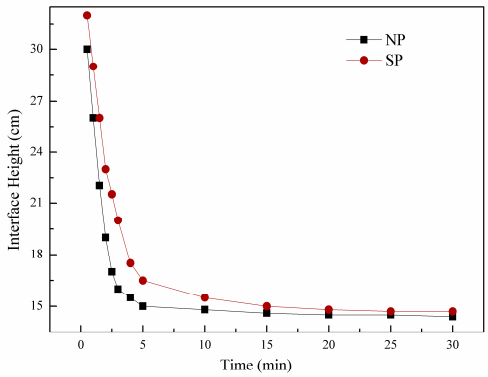

Figure 13 Floc settling behavior of flocculants

Preprints (www.preprints.org) | NOT PEER-REVIEWED | Posted: 1 August 2018 doi:10.20944/preprints201808.0005.v1

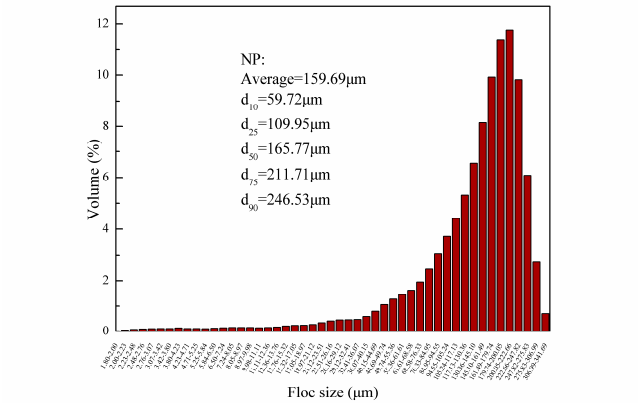

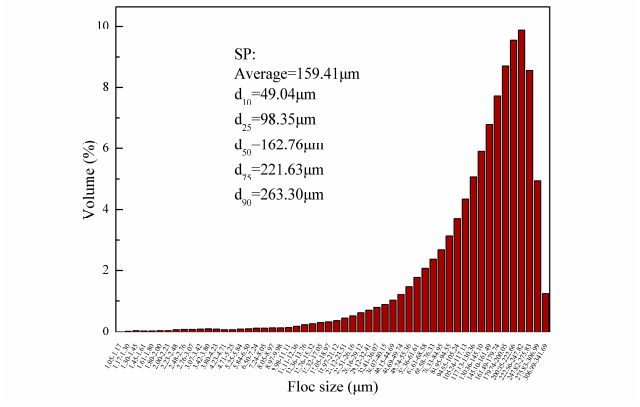

Figure 14 Floc size distribution for (a) NP and (b) SP

To examine the effects of the novel UV initiation system on flocculant sludge conditioning mechanism, floc characteristics, such as settling behavior and floc size distribution with NP and SP, were comparatively investigated. Figure 13 plots the settling rate of sludge, which is expressed in terms of height of sludge–water interface as a function of time, with the dosage of various flocculants controlled at 40 mg/L. In this study, the rate of sludge–water interfacial height variation over 5 min was assumed to be the sludge sedimentation rate. Settling rates reached 4.0 and 3.7 cm/min for the sludge conditioned with NP and SP, respectively. A better settling capability of NP can be observed. At the end of settling, similar heights of 14.4 and 14.7 cm were achieved for NP and SP, respectively. These findings indicate the similar floc sizes of sludge particles conditioned by NP and SP. Nearly the same average floc size of the two polyelectrolytes can be estimated in Figure 14. The different settling behavior may be attributed to floc density and floc size distribution. As shown in Figure 14, d_{10} and d_{25} of NP were higher than those of SP, indicating that less small floc particles existed in NP-conditioned sludge. Few small particles favored sludge dewatering because the cloth filter was less likely to be clogged[31]. This condition may imply the low SRF of NP, as shown in Figure 12. However, d_{75} and d_{90} of NP were smaller than those of SP. Bridging played a prominent role in sludge conditioning for SP as bridging mechanism is constantly characterized with large floc size[32]. However, such large floc size can be disadvantageous for sludge dewatering. Previous studies examined that large and loose flocs with high content of intrafloc water (water from within the floc, comprising loops and tails)[33], which is not easily removed during filtration, were formed. This phenomenon corresponded well with the high FCMC of SP, as indicated in Figure 12.

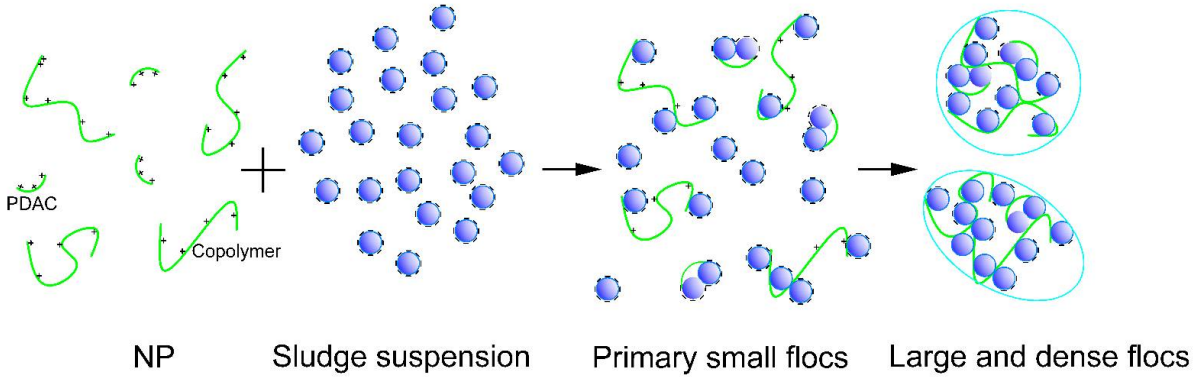

Figure 15. Sludge flocculation mechanism scheme of NP

The different initiation systems included the origin of different sludge conditioning performances and mechanisms. Figure 15 shows sludge flocculation scheme of NP. As it was shown in Figure 3, several fractions of PDAC existed in NP. After the addition of NP, the sludge particles were neutralized and destabilized with the existence of PDAC and copolymers and. At such condition, the main flocculation mechanism was charge neutralization given that the strength between charged sites is frequently higher than Van der Waals force or hydrogen bond[7_ENREF_7]. Flocs are assumed to form through charge neutralization and are characterized with compactness and low intrafloc water. However, numerous negative sites were still found on sludge particles as the zeta potential was lower than 0 mV at a dosage of 40 mg/L, as shown in Figure 12 (a). Bridging became the main flocculation mechanism to form large and dense sludge flocs through Van der Waals force, hydrogen bond, or electrical force. This condition may explain the floc size distribution and sludge conditioning performance of NP. On the contrary, in the single initiator and stable light intensity system, DAC monomers were not sufficiently reacted, the first step of charge neutralization cannot function well, and bridging serves as the main mechanism during flocculation. We observed that flocs mainly formed through bridging were loose and featured a wide range of floc size distribution and high percent of intrafloc water. Therefore, the sludge conditioning performance of SP was poorer than that of NP.

5. Conclusions

In this study, a novel UV-initiated system characterized with adjustable light intensity and redox-azo complex initiator to maintain a certain concentration of free radicals was used to synthesize NP. The parameters affecting intrinsic viscosity, conversion, and dissolving time of NP were studied. The structure, morphology, and thermal stability were investigated using FT-IR, ^{1}H NMR, TG-DSC, and SEM. Finally, sludge conditioning performance and mechanism of NP were investigated. On the basis of experimental results, the following conclusions were obtained:

(1) Characterization results indicated that NP was successfully prepared with AM and DAC by FT-IR and ^{1}H NMR spectra. ^{1}H NMR spectra indicated that a small fraction of PDAC was mixed in NP. An accepted thermal stability was examined by TG-DSC. Surface morphology of NP characterized by SEM showed that a porous structure was observed, and an acceptable dissolvability and a stronger adsorption-bridging behavior were noted between sludge particles and polymer molecules.

(2) NP exhibited the best complex performance at intrinsic viscosity, conversion rate, and dissolving time at 0.45 wt‰ redox initiator concentration, 0.2 wt‰ azo initiator concentration, 40.0 wt% CD, first- and second-stage light intensities of 8.5 and 13 mW/cm^2, respectively, and 3 wt% urea,. The advantages of the novel UV initiation system over stable light intensity and single initiator were analyzed. Radical concentrations were maintained as redox initiators decomposed at low activation energy, and azo initiators were generated at high activation energy.

(3) The sludge conditioning experiment showed that NP performed better in terms of RT, FCMC, and SRF than SP. A flocculation mechanism was proposed by investigating the sedimentation behavior and floc size distribution. High intrinsic viscosity, porous morphology structure, and mixed cationic homopolymer of NP contributed to good sludge conditioning performances.

Author Contributions: Qingqing Guan, Guocheng Zhu and Yi Liao conceived and designed the experiments; Jin Xu, Xiaoxu Sun and Fang Tian performed the experiments; Minghan Luo and Jiaxing Xu analyzed the data; every author contributed to writing the paper.

Funding: The authors are grateful for the financial support provided by the Natural Science Foundation of Jiangsu (Project BK20160779), Natural Science Research of Jiangsu Universities (Project 16KJB610008), Academic Research Foundation of Nanjing Institute of Technology (Project YKJ201527), the Department of Science and Technology of Sichuan Province (Project No. 2017JY0129) and the Education Committee of Sichuan Province (Project No.17ZB0312).

Conflicts of Interest: The authors declare no conflict of interest.

References

1. Nguyen, T.P.; Hilal, N.; Hankins, N.P.; Novak, J.T. Characterization of synthetic and activated sludge and conditioning with cationic polyelectrolytes. *Desalination* **2008**, *227*, 103-110.
2. Ma, M.; Zhu, S. Grafting polyelectrolytes onto polyacrylamide for flocculation 2. Model suspension flocculation and sludge dewatering. *Colloid Polym. Sci.* **1999**, *277*, 123-129.
3. Wolski, P.; Zawieja, I. Hybrid conditioning before anaerobic digestion for the improvement of sewage sludge dewatering. *Desalin. Water Treat.* **2014**, *52*, 3725-3731.
4. Zhu, J.; Zheng, H.; Jiang, Z.; Zhang, Z.; Liu, L.; Sun, Y.; Tshukudu, T. Synthesis and characterization of a dewatering reagent: Cationic polyacrylamide (p(am-dmc-dac)) for activated sludge dewatering treatment. *Desalination and Water Treatment* **2013**, *51*, 2791-2801.
5. Zheng, H.; Sun, Y.; Zhu, C.; Guo, J.; Zhao, C.; Liao, Y.; Guan, Q. Uv-initiated polymerization of hydrophobically associating cationic flocculants: Synthesis, characterization, and dewatering properties. *Chemical Engineering Journal* **2013**, *234*, 318-326.
6. Zheng, H.; Liao, Y.; Zheng, M.; Zhu, C.; Ji, F.; Ma, J.; Fan, W. Photoinitiated polymerization of cationic acrylamide in aqueous solution: Synthesis, characterization, and sludge dewatering performance. *The Scientific World Journal* **2014**, *2014*, 1-11.
7. Bolto, B.; Gregory, J. Organic polyelectrolytes in water treatment. *Water Research* **2007**, *41*, 2301-2324.
8. Zheng, H.; Sun, Y.; Guo, J.; Li, F.; Fan, W.; Liao, Y.; Guan, Q. Characterization and evaluation of dewatering properties of padb, a highly efficient cationic flocculant. *Industrial & Engineering Chemistry Research* **2014**, *53*, 2572-2582.
9. Zhou, J.; Liu, F.; Pan, C. Effects of cationic polyacrylamide characteristics on sewage sludge dewatering and moisture evaporation. *PLoS ONE* **2014**, *9*, e98159.
10. Guan, Q.; Zheng, H.; Zhai, J.; Liu, B.; Sun, Y.; Wang, Y.; Xu, Z.; Zhao, C. Preparation, characterization, and flocculation performance of p(acrylamide-co-diallyldimethylammonium chloride) by uv-initiated template polymerization. *Journal of Applied Polymer Science* **2015**, *132*, 10.1002/app.41747.
11. Shang, H.; Zheng, Y.; Liu, J. Synthesis in inverse emulsion and decolorization properties of hydrophobically modified cationic polyelectrolyte. *Journal of Applied Polymer Science* **2011**, *119*, 1602-1609.
12. Ma, J.; Zheng, H.; Tan, M.; Liu, L.; Chen, W.; Guan, Q.; Zheng, X. Synthesis, characterization, and flocculation performance of anionic polyacrylamide p (am-aa-amps). *Journal of Applied Polymer Science* **2013**, *129*, 1984-1991.
13. Agarwal, V.; McLean, D.; Horne, J.; Richardson, D.; Stack, K. Chemometric study of graft copolymerization of guar-g-(acrylamide-co-diallyl dimethylammonium chloride). *Journal of Applied Polymer Science* **2013**, *127*, 3970-3979.
14. Zhao, S.-M.; Liu, K.-Y. Synthesis of copolymer of dmdaac and am. *Beijing Huagong Daxue Xuebao (Ziran Kexueban)/Journal of Beijing University of Chemical Technology (Natural Science Edition)* **2005**, *32*, 29-32.
15. Bamford, C.H. 9 - redox initiators a2 - allen, geoffrey. In *Comprehensive polymer science and supplements*, Bevington, J.C., Ed. Pergamon: Amsterdam, 1989; pp 123-139.
16. Pabin-Szafko, B.; Wisniewska, E.; Hefczyc, B.; Zawadiak, J. New azo-peroxidic initiators in the radical polymerization of styrene and methyl methacrylate. *European Polymer Journal* **2009**, *45*, 1476-1484.

17. Sun, Y.; Zhu, C.; Xu, Y.; Zheng, H.; Xiao, X.; Zhu, G.; Ren, M. Comparison of initiation methods in the structure of cpam and sludge flocs properties. *Journal of Applied Polymer Science* **2016**, *133*, n/a-n/a.
18. Guan, Q.; Zheng, H.; Zhai, J.; Zhao, C.; Zheng, X.; Tang, X.; Chen, W.; Sun, Y. Effect of template on structure and properties of cationic polyacrylamide: Characterization and mechanism. *Industrial & Engineering Chemistry Research* **2014**, *53*, 5624-5635.
19. Guan, Q.; Zheng, H.; Xu, J.; Tian, F.; Sun, X. Effect of charge density on structural characteristics of cationic polyacrylamide: Models based on reactivity ratio and characterization. *Journal Of Polymer Materials* **2016**, *33*, 365-377.
20. Guan, Q.; Tang, M.; Zheng, H.; Teng, H.; Tang, X.; Liao, Y. Investigation of sludge conditioning performance and mechanism by examining the effect of charge density on cationic polyacrylamide microstructure. *Desalination and Water Treatment* **2016**, *57*, 12988-12997.
21. Abdollahi, Z.; Frounchi, M.; Dadbin, S. Synthesis, characterization and comparison of pam, cationic pdmc and p(am-co-dmc) based on solution polymerization. *Journal of Industrial and Engineering Chemistry* **2011**, *17*, 580-586.
22. Feng, L.; Zheng, H.; Gao, B.; Zhao, C.; Zhang, S.; Chen, N. Enhancement of textile-dyeing sludge dewaterability using a novel cationic polyacrylamide: Role of cationic block structures. *Rsc Advances* **2017**, *7*, 11626-11635.
23. Ma, J.; Shi, J.; Ding, H.; Zhu, G.; Fu, K.; Fu, X. Synthesis of cationic polyacrylamide by low-pressure uv initiation for turbidity water flocculation. *Chemical Engineering Journal* **2017**, *312*, 20-29.
24. Seabrook, S.A.; Gilbert, R.G. Photo-initiated polymerization of acrylamide in water. *Polymer* **2007**, *48*, 4733-4741.
25. Yuan, Z.; Hu, H. Preparation and characterization of crosslinked glyoxalated polyacrylamide paper-strengthening agent. *Journal of Applied Polymer Science* **2012**, *126*, E458-E468.
26. Liu, L.Y.; Yang, W.T. Inverse emulsion polymerization of acrylamide initiated by uv radiation. *Acta Polymerica Sinica* **2004**, 545-550.
27. Yoon, D.H.; Jang, J.W.; Cheong, I.W. Synthesis of cationic polyacrylamide/silica nanocomposites from inverse emulsion polymerization and their flocculation property for papermaking. *Colloids and Surfaces A: Physicochemical and Engineering Aspects* **2012**, *411*, 18-23.
28. Yang, Z.; Liu, X.; Gao, B.; Zhao, S.; Wang, Y.; Yue, Q.; Li, Q. Flocculation kinetics and floc characteristics of dye wastewater by polyferric chloride–poly-epichlorohydrin–dimethylamine composite flocculant. *Separation and Purification Technology* **2013**, *118*, 583-590.
29. Saveyn, H.; Meersseman, S.; Thas, O.; Van der Meeren, P. Influence of polyelectrolyte characteristics on pressure-driven activated sludge dewatering. *Colloids and Surfaces A: Physicochemical and Engineering Aspects* **2005**, *262*, 40-51.
30. Chen, Q.; Wang, Y. Influence of single- and dual-flocculant conditioning on the geometric morphology and internal structure of activated sludge. *Powder Technology* **2015**, *270, Part A*, 1-9.
31. Feng, L.; Liu, S.; Zheng, H.; Liang, J.; Sun, Y.; Zhang, S.; Chen, X. Using ultrasonic (us)-initiated template copolymerization for preparation of an enhanced cationic polyacrylamide (cpam) and its application in sludge dewatering. *Ultrasonics Sonochemistry* **2018**, *44*, 53-63.
32. Zhao, C.; Zheng, H.; Feng, L.; Wang, Y.; Liu, Y.; Liu, B.; Djibrine, B.Z. Improvement of sludge dewaterability by ultrasound-initiated cationic polyacrylamide with microblock structure: The role of surface-active monomers. *mater.* **2017**, *10*.
33. Xiao, J.; Wu, X.; Yu, W.; Liang, S.; Yu, J.; Gu, Y.; Deng, H.; Hu, J.; Xiao, K.; Yang, J. Migration and distribution of sodium ions and organic matters during electro-dewatering of waste activated sludge at different dosages of sodium sulfate. *Chemosphere* **2017**, *189*, 67-75.